Journal of Iberian Geology
[illegible]doi.org[illegible]

[illegible]

Primary phosphate mineralization in mandibular elements of middle paleozoic archaeostracans from Spain

Mónica Martí Mus[1] · **Victor López-Rojas**[2,3]

[illegible] July [illegible] November [illegible]

Abstract

Archaeostracans are an early fossil crustacean group linked to malacostracans. The earliest archaeostracans are late Cambrian, but the group diversified mostly in the Silurian and Devonian. Complete specimens are known from konservat-lagerstätten, but loose mandibular elements are relatively abundant in decalcified, acid resistant residues of middle Palaeozoic carbonates. These mandibular elements have been assumed to be originally heavily sclerotized and secondarily phosphatized, but have received little attention in the scientific literature. In the present study, we describe isolated mandibular elements, gnathal lobes (likely belonging to a single archaeostracan species), from the middle Palaeozoic of the Cordoba Province, Spain, and provide evidence that they were originally mineralized with calcium phosphate. Our results are in accordance with recent evidence that malacostracans use calcium phosphate to strengthen mechanically challenged areas of their cuticle, particularly the wear prone mandibular surfaces, and support the hypothesis of a dual calcium phosphate/carbonate mineralization system evolving early in arthropods.

Resumen

Los arqueostracos son un grupo de crustáceos fósiles tempranos relacionados con los malacostráceos. Los primeros arqueostracos son del Cámbrico tardío, pero el grupo se diversificó sobre todo en el Silúrico y el Devónico. Se conocen ejemplares completos procedentes de yacimientos de preservación excepcional, pero los elementos mandibulares sueltos son relativamente abundantes en residuos de carbonatos del Paleozoico medio disueltos en ácidos débiles. Se ha supuesto que estos elementos estaban originalmente esclerotizados y se fosfatizaron secundariamente, pero han recibido poca atención en la literatura científica. En el presente estudio describimos elementos mandibulares aislados, lóbulos gnatales (probablemente pertenecientes a una única especie de arqueostraco), procedentes del Paleozoico medio de la región de Córdoba, España, y aportamos pruebas de que estaban originalmente mineralizados con fosfato cálcico. Nuestros resultados concuerdan con datos recientes que muestran que los malacostraceos utilizan el fosfato cálcico para reforzar zonas de su cutícula sometidas a retos mecánicos, en particular las superficies mandibulares, propensas al desgaste. Nuestros resultados apoyan la hipótesis de que un sistema dual de mineralización, que usaba fosfato y carbonato cálcico, evolucionó tempranamente en los artrópodos.

Palabras Clave Biomineralización · Arqueostracos · Crustáceos · Malacostráceos · Artrópodos tempranos · Fosfato · Cutícula de artrópodos · Microestructura

Keywords Biomineralization · Archaeostracans · Crustaceans · Malacostracans · Early arthropods · Phosphate · Arthropod cuticle · Microstructure

✉ Mónica Martí Mus
martimus@unex.es

Victor López-Rojas
v.rojas@campus.fct.unl.pt

1 Área de Paleontología, Universidad de Extremadura, Avenida de Elvas s/n, Badajoz 06006, Spain

2 GeoBioTec, FCT-UNL, Faculdade de Ciências e Tecnologia, Universidade Nova de Lisboa, Portugal, 2829-516 Monte da Caparica, Portugal

3 Museu da Lourinhã, Rua João Luís de Moura, 95, Lourinhã 2530-158, Portugal

Published online: 20 December 2024

1 Introduction

Archaeostracans are an early fossil crustacean group usually linked to malacostracans. The earliest archaeostracans are Cambrian (Furongian; Collette & Hagadorn, 2010a), but the group diversified mostly in the Silurian and Devonian (Rolfe, 1969; Collette & Hagadorn, 2010b). Occurrences of well-preserved, complete individuals are relatively rare (e.g. Briggs et al., 2004, 2011; Collette & Hagadorn, 2010a; Collette & Rudkin, 2010; Jones et al., 2015; Broda et al., 2017), but they occur abundantly as disarticulated mandibular elements in acid resistant residues of middle Palaeozoic carbonate rocks treated with acetic acid (Dzik, 1980). This methodology is widely used to extract phosphatic fossils, such as conodonts and fish remains in general, but also diverse secondarily phosphatized fossils. Archaeostracan mandibles (their isolated gnathal lobes, see below) are relatively common in this kind of sample, but have received little attention historically, and, while the presence of phosphate in them has been previously noted (Dzik, 1980; Schülke & Riemann, 2002), it has been assumed to be secondary, of diagenetic origin (Dzik, 1980). Phosphate has also been noted numerous times in the archaeostracan cuticle, but also commonly assumed to be diagenetic (e.g. Vannier et al., 2003, Briggs et al., 2011; Jones et al., 2015; Broda et al., 2017, Liu et al., 2023), although not always (e.g. Rolfe, 1962; Wendruff et al., 2020). However, recent studies on modern malacostracans have shown that the cuticle of their mandibles is locally hardened with calcium phosphate, and that this trait is widely distributed among the group, suggesting it is an inherited trait which evolved early in the crustacean lineage (Bentov et al., 2012, 2016a, b; the presence of phosphate in the crustacean cuticle has long been known, see early reviews in Richards, 1951, pp. 100–104, and Rolfe, 1962, pp. 34–35). Stemming from these observations and what is generally known about the presence of phosphate in the mineralized cuticle of crustaceans, it has also been argued (Bentov et al., 2016a) that crustaceans may have a phylogenetically old, "dual" biomineralization system able to produce various minerals along the calcium carbonate-calcium phosphate spectrum.

In the present study, we describe isolated gnathal lobes (likely belonging to a single archaeostracan species) from the middle Palaeozoic of the Cordoba Province, Spain, and provide evidence that they were originally mineralized with calcium phosphate, supporting the hypothesis of a dual calcium phosphate/carbonate mineralization system evolving early in the arthropod lineage (Bentov et al., 2016a).

2 Archaeostracans and archaeostracan mandibles

Archaeostracans are phylogenetically linked to malacostracan crustaceans. Malacostracan detailed phylogeny is controversial, but the monophyly of the group is generally accepted (see review in Richter et al., 2009; Schwentner et al., 2018). In present day Malacostraca there are the anatomically distinct, shrimp-like leptostracans, a small group generally retrieved as the sister group of the rest of malacostracans (the Eumalacostraca). Fossils that resemble present-day leptostracans have been known since the 19th century, and were originally included, together with present-day leptostracans, in the Subclass Phyllocarida (Packard, 1879). The Phyllocarida was later separated into the orders Leptostraca (Claus, 1880), for the extant species, and Archaeostraca (Claus, 1888) for the fossils. Archaeostracans share with leptostracans several characters, such as the possession of a bivalved carapace and the number of segments in the thorax and abdomen (Rolfe, 1969). However, depending on the final topology of the malacostracan tree, these features could be plesiomorphic for the clade Malacostraca, questioning the group Phyllocarida and making the phylogenetic position of archaeostracans uncertain (Hessler & Schram, 1984). Taking also into account their early occurrence, archaeostracans could represent a paraphyletic assemblage, potentially distributed along any or all of the Malacostraca, Eumalacostraca and Leptostraca stem groups (see Rolfe, 1981).

Malacostracans possess 3 pairs of mouth appendages, referred to from front to back as mandibles, maxillules and maxilla. The mandibles are highly specialized for food manipulation and usually possess a mandibular palp and a gnathal lobe. The gnathal lobe develops as a serrated extension of the coxa, and is usually strongly mineralized in present day malacostracans. The gnathal lobes of the right and left mandibles face each other in front of the mouth and are used to manipulate (chew, dismember, etc.) food. The gnathal lobe is differentiated into a wider, flattened molar part and a dentated incisor part. This differentiation could be phylogenetically very old, as the mandibles themselves, and a shared homology for all mandibulates (Edgecombe et al., 2003). The mandibular palp, arising also from the coxa, corresponds to the endopodite of the biramous appendage and may be highly modified. The mandible of archaeostracans is similar to that of present day malacostracans. It has a mandibular corpus (the coxa) and a gnathal lobe diferentiated into molar and incisor parts (Rolfe, 1969; Dzik, 1980).

3 Mineralization of the cuticle in modern crustaceans and in archaeostracans

Crustaceans have a layered external cuticle, generally mineralized to varying degrees with amorphous calcium carbonate, and minor amorphous calcium phosphate. These two components form a "solid solution" along the cuticle with varying PO_4/CO_3 ratios (Bentov et al., 2016a). It is believed that calcium phosphate is mostly used to prevent the crystallization of the amorphous calcium carbonate. However, it has been recently shown that, in malacostracans, calcium phosphate is also used selectively to strengthen mechanically challenged areas of the cuticle, both in its amorphous phase and as crystalline fluorapatite (Bentov et al., 2016a, b). Some of these areas are the wear prone mandibular surfaces, which in the most elaborate examples have a distinct fluorapatite coating (Bentov et al., 2012, 2016b). Bentov et al. (2016a) have further argued that crustaceans have a versatile, "dual" biomineralization system able to produce various minerals along the calcium carbonate-calcium phosphate spectrum (namely calcite, amorphous calcium carbonate, amorphous calcium phosphate and apatite). Bentov et al. (2016a) have also argued that crustaceans are able to "fine tune" their dual biomineralization system to form structures with different mechanical properties and that, given its widespread distribution in crustaceans, this dual system likely originated early in the history of the group. This observations and model may be consistent with palaeontological data. The gnathal lobes of archaeostracan mandibles characteristically survive acetic acid dissolution, and are generally assumed to be phosphatic (Dzik, 1980). Schülke and Riemann (2002) also reported the presence of an enamel-like cap, covering the tip of the denticles in various mandibular elements. However, no chemical data was presented in either of the above studies to back phosphatic composition of the mandibles. Phosphate has also been repeatedly reported (and documented with chemical data) from archaeostracan cuticle (e.g. Vannier et al., 2003: Briggs et al., 2011; Jones et al., 2015; Liu et al., 2023). Also, numerous early arthropod fossils with phosphatic cuticles have been described. Some of these early arthropods (e.g. phosphatocopines, aglaspidids; see Lin et al., 2011 for a review of phosphatic early arthopods) are currently accepted as originally phosphatic but, in general, the difficulty to distinguish original from diagenetic phosphatization in extinct forms has rendered the topic controversial.

4 Materials and methods

The studied fossils come from loose blocks of limestone collected southwest of Puerto Calatraveño, north-western part of Sierra Morena, Cordoba Province (Fig. 1a, b). With respect to the tectonostratigraphic division of the

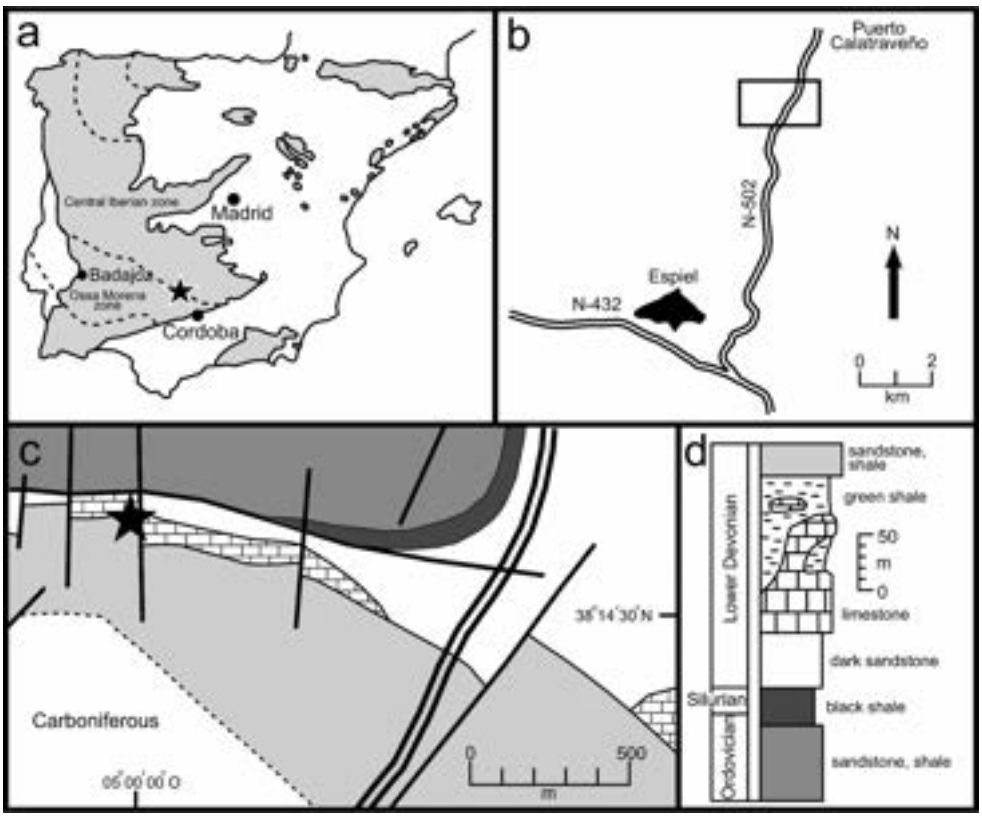

Fig. 1 Provenance of the studied material. **a** Map of the Iberian Peninsula showing tectonostratigraphical subdivision and location of study area, indicated by a star, close to the boundary between the Ossa Morena and Central Iberian zones. **b** Location of study area, some 6.5 km north of the village Espiel. Rectangle indicates area shown in **c**. **c** Geology of the study area (based on Apalategui Isaza et al., 1985b and Mapa Continuo 1:50.000 del Instituto Geológico y Minero; info.igme.es/visor/), showing location of studied blocks south of lower Devonian carbonates. **d** Stratigraphic column of study area based on Apalategui Isaza et al. (1985b). Dissolved limestone blocks may have originated from the lower Devonian carbonates

Iberian Peninsula the area belongs to the Ovejo-Valsequillo domain, with a position intermediate between the Ossa Morena and Central Iberian Zones (Fig. 1a). This is a structurally complex area with abundant thrusts and faults. Some of the limestone blocks are fine-grained and black in fresh cut, weathering ochre; others contain a higher proportion of siliciclastic material. The limestone blocks contain macrofauna that includes crinoids and orthocone cephalopods. According to their geographic location relative to the most recent geological map of the area (Apalategui Isaza et al., 1985b), these blocks could belong to a lower Devonian carbonate unit that crops out immediately to the north (Fig. 1c, d), and which has a highly variable development within the region (Apalategui Isaza et al., 1985a. However, the fauna described from this limestone unit in Apalategui Isaza et al. (1985a) differs from that encountered in the collected blocks and further studies are necessary to confirm their precise stratigraphical provenance.

Fossils were isolated from the carbonate matrix using the acetic acid maceration technique described in Jeppsson et al. (1999). Specimens were imaged using scanning electron microscopy (with both secondary and backscattered electron detectors). Energy dispersive X-ray spectroscopy (EDS) and backscattered electron (BSE) imaging were used in combination to analyse the elemental (and infer the mineral) composition of the fossils. Since in BSE images the contrast depends mostly on the atomic number of the elements in the sample (with elements with higher atomic numbers appearing brighter), the combination of EDS and BSE imaging provides a precise map of the distribution of the different minerals on the specimens. All studied specimens were analysed with EDS and BSE imaged. SEM imaging and EDS where carried out on a Hitachi FE-SEM S-4800 and a FEI Quanta 3D FEG at "Servicio de análisis y caracterización de sólidos y superficies de la Universidad de Extremadura", Badajoz (Spain). Illustrated fossils are housed in the collections of Área de Paleontología, Universidad de Extremadura, Badajoz, Spain.

5 Results and discussion

The studied specimens represent isolated gnathal lobes of archaeostracan mandibles. All are very similar (Figs. 2, 3a–e, 4 and 5a), suggesting they all belong to the same species, likely *Ceratiocaris bohemicus*, which has been reported from the same general area (Lorenzo et al., 2020).

The fossils are all fragmentary to some extent, the most complete ones being those illustrated in Figs. 2a and 5a (same specimen), 2 h and i (same specimen), 2k and 2 L. They are preserved as a relatively thin, concavo-convex plate, therefore, the teeth are not solid but form deep cavities on the internal surface (Fig. 3a–f). There are specimens belonging both to left (Figs. 2f and k and 3c) and right (Figs. 2a, d, g–j and l and 3a, b, d and e) mandibles. Specimens in Fig. 2c and e are too fragmentary to assess their curvature and therefore infer their location in the body. Right and left mandibles are mirror images of each other in terms of curvature, but not in the arrangement of teeth and molar part (e.g., the "extended margin" of the molar part is on the convex side in the right mandible, but in the concave side in the left mandible; compare specimens in Fig. 2k and l). The following detailed description focuses mostly on the morphology of the right mandible, since they appear to be more abundant (or better preserved) in our samples. The gnathal lobes have a short molar part, consisting of a flat, thinly ridged, subtriangular platform (Figs. 2b, d, g, j, k and l and 3a–c, e and g). On both external and internal surfaces, it can be appreciated that one of the margins of the molar part extends further into the toothed portion of the mandible than the other (Figs. 2g and j and 3a–c and e). Externally, the ridges are more apparent along this extended margin (Fig. 2b, d, g, j, m). The molar part leads to a central zone with connected teeth forming a zigzag pattern (Figs. 2a, b, d, f and g–l and 3a–e). Repeated tricuspid units, consisting of three pointed teeth connected by thin crests, form the zigzag pattern (Dzik, 1980, p. 94; Figs. 2a, d and f–l and 3b and e). Towards the distal end, the gnathal lobe gradually narrows, the teeth become longer, and the tricuspid pattern blurs leading to paired conical, fang-like teeth (Fig. 2c, e, h, i, k). The complete incisor part (the entire toothed part) seems to consist of six sets of teeth (perhaps 7 in some specimens; Fig. 3a, b), each set with a characteristic morphology and gradually increasing in height towards the distal end. Only three sets of teeth in the median region (numbered 3, 4 and 5; Figs. 2a, d and f–l and 3a–c and e) show a clear tricuspid pattern (although a third tiny tooth can also be distinguished associated with the two distal, fang-like sets of teeth; Fig. 2e). Teeth nº 6 (and also nº 7 when it is present) is small and faces (appears interrupted by) the extended margin of the molar part (Figs. 2g, j, k and l and 3a–c and e). A pitted pattern can be observed laterally, on the base of the gnathal lobe of some specimens (Fig. 2d, j). Regarding the internal surface of the lobes, thin, regularly spaced transverse ridges occur on the molar part, which together with perpendicular (perhaps more internal) lines form a quadrangular reticulation (Fig. 3a–c, e, g). The reticulation becomes fan-like (radiating) in the margin of the molar part that extends into the incisor part (Fig. 3e, f), and shows a honeycomb pattern on the internal surface of teeth (Fig. 3f).

The microstructure of the gnathal lobes is layered and fibrous. Layering is more apparent at the base of the lobes (Fig. 3a, d, f, h) and less obvious on the teeth themselves, which instead expose a conspicuous fibrous microstructure

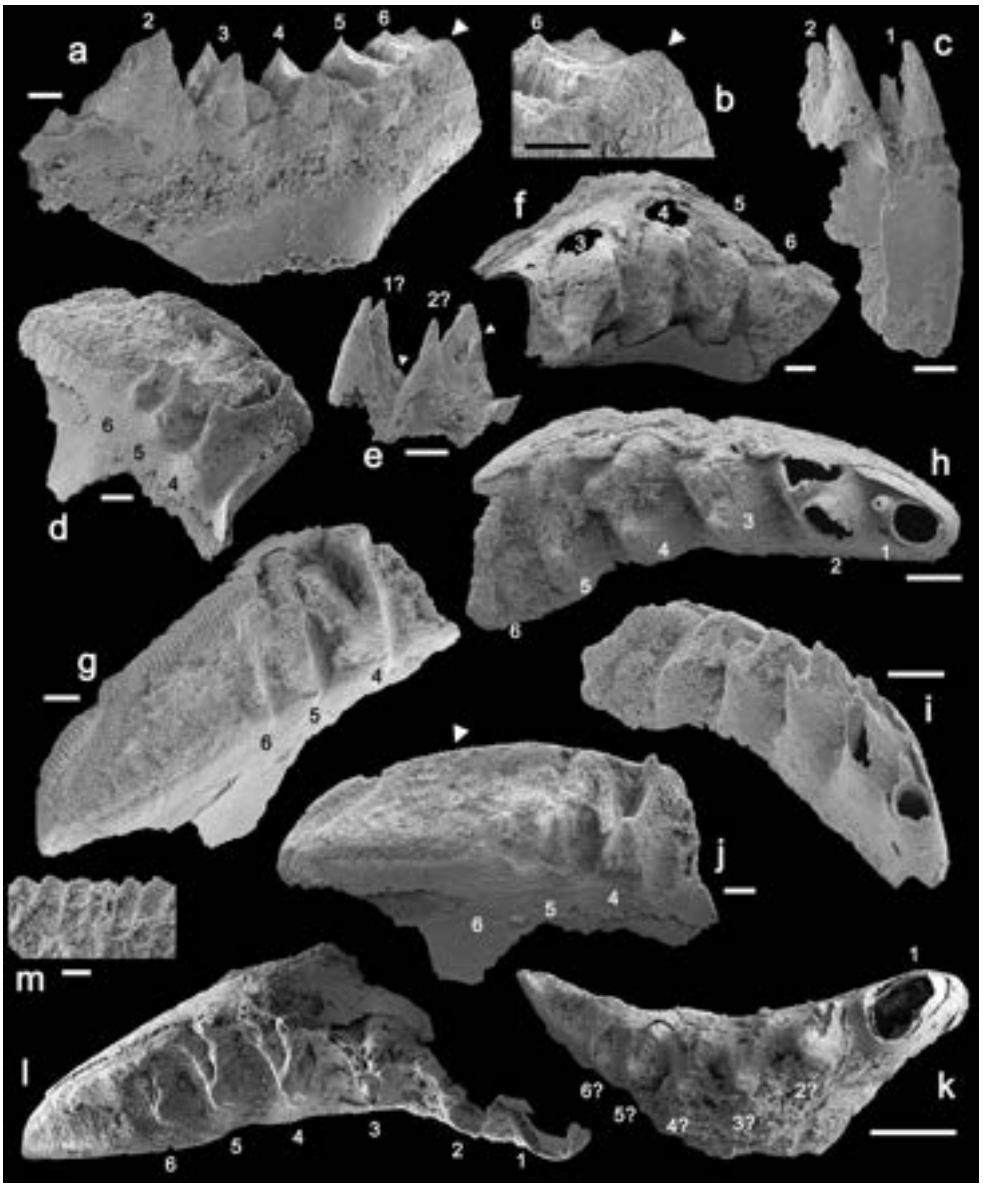

Fig. 2 General morphology of isolated archaeostracan gnathal lobes, external surface view; from Puerto Calatraveño area. All images were taken under SEM, and all are Secondary Electron (SE) images. All specimens are fragmentary to some extent; the most complete ones are those illustrated in k (left mandible), and l (right mandible). Specimens illustrated in f and k are left mandibles, those illustrated in a, d, g–j and l are right mandibles. Specimens in c and e are too fragmentary to assess their curvature and therefore infer their location in the body. **a** Specimen UEXP880Pu1:012; both extremes of the lobe are missing. **b** Close up of specimen UEXP880Pu1:012, to show ribbing (arrowed; also arrowed in **a**) that marks the start of the molar part. **c** Specimen UEXP880Pu1:021; incisor part of lobe with the first two sets of teeth preserved; note fang-like morphology. **d**, **g**, **j**, **m** Specimen UEXP880Pu1:018 in different views; specimen with complete molar part, to the left, and last sets of teeth preserved; note transverse ridges in the margins of the molar part (more noticeable on the convex margin; enlarged in **m**) and pitted lateral surface on the concave margin (more visible in **d** and **j**); note also the morphology of the tricuspid units; arrowhead in **j** marks area enlarged in **m**. **e** Specimen UEXP880Pu1:033; fragment of lobe showing sets of teeth 1? and 2?; note fang-like morphology, but also tricuspid organization with very small third teeth (arrowed). **f** Specimen UEXP880Pu1:017; middle portion of the gnatal lobe preserved; note morphology of tricuspid units. **h**, **i** Specimen UEXP880Pu1:025 in occlusal and lateral views respectively; gnathal lobe with complete incisor part, molar area is missing to the left of the specimen. **k** Specimen UEXP880Pu1:036, almost complete left mandible. **l** Specimen UEXP880Pu1:037, almost complete right mandible. Numbering (from 1 to 6) identifies sets of (tricuspid) teeth starting at the incisor end. Scale bars represent 100 μm in **a**–**j**; scale in **k** represents 500 μm for **k** and **l**; scale in **m** represents 20 μm

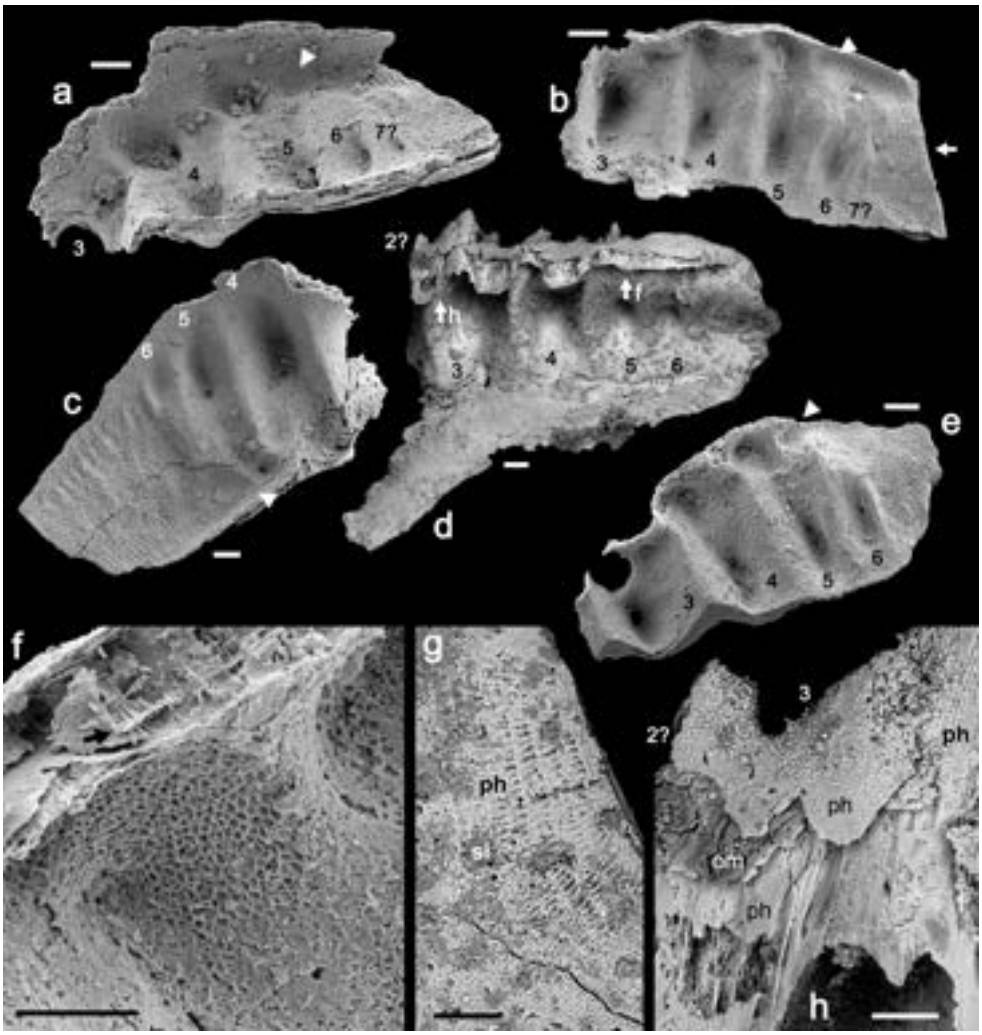

Fig. 3 General morphology, structure and composition of isolated archaeostracan gnathal lobes from Puerto Calatraveño area. All specimens except that in **h** show underside of lobe. All images were taken under SEM. Images **a**–**c**, **e** and **f** are SE images; those in **d**, **g** and **h** are BSE images. Specimen in **c** is a left mandible, the rest are right mandibles. All specimens show last sets of teeth and incomplete molar part; note how the margin of the molar part extends further on one of the sides (arrowheads in **a**–**c** and **e**); note also fine ribbing and small pores on molar part (specimens in **a**–**c**, **e** and **g**). **a** Specimen UEXP880Pu1:011; note layered structure of the gnathal lobe; the specimen appears to have two small teeth (6 and 7?) opposite the "extended margin" of the molar part (arrowhead). **b** Specimen UEXP880Pu1:016, also appears to have two small teeth (6 and 7?) opposite the "extended margin" of the molar part (arrowhead); arrow points to area enlarged in **g**. **c** Specimen UEXP880Pu1:010. **d** Specimen UEXP880Pu1:006; note layered structure (see enlarged areas, arrowed, in h and f); The bulk of the specimen is composed of calcium phosphate (light grey); darker grey dots are small silica patches; a darker layer of organic matter is also visible (better seen in **h**). **e** Specimen UEXP880Pu1:002; note slightly radiating ribbing on "exteded margin" of molar part (arrowhead). **f** Detail of specimen UEXP880Pu1:006 (see arrow in **d**); honeycomb reticulation in underside of teeth (left of the image) and somewhat radiating reticulation in "extended margin" of molar part (right of the image); note also layered and fibrous structure in the margin of the lobe, with thin fibres cutting across a thin perpendicular layer (arrow). **g** Specimen UEXP880Pu1:016; enlarged area of molar part (see arrow in **b**), note quadrangular reticulation. The bulk of the specimen is phosphatic (ph) in composition, darker patches are siliceous (si). **h** Detail of specimen UEXP880Pu1:006 (see arrow in **d**); lateral surface of specimen illustrating layered and fibrous structure; dark, cracked laye is composed of organic matter (om), the rest of layers and fibres are composed of calcium phosphate (ph). Numbering (from 1 to 7) identifies sets of (tricuspid) teeth starting at the incisor end. Scale bars represent 100 μm in **a**–**e** and 50 μm in **f**–**h**. Abbreviations: om: organic matter; ph: calcium phosphate; si: silica/ phyllosilicates

(Fig. 4). Fibres are long and mostly oriented vertically (along the teeth longest dimension). They vary in thickness and appear hierarchically organized, with thicker fibres consisting of bundles of thinner ones (Fig. 4e, f). In some specimens, bundles of fibres clearly cut across thin horizontal/oblique layers that appear perforated by pores through which the fibres emerge (Figs. 3f and 4f). The observed fibrous microstructure is similar to that of modern crustaceans (e.g. compare Fig. 4f, with Fig. 6a of Cheng et al., 2008), which reflects the organization of chitin fibres.

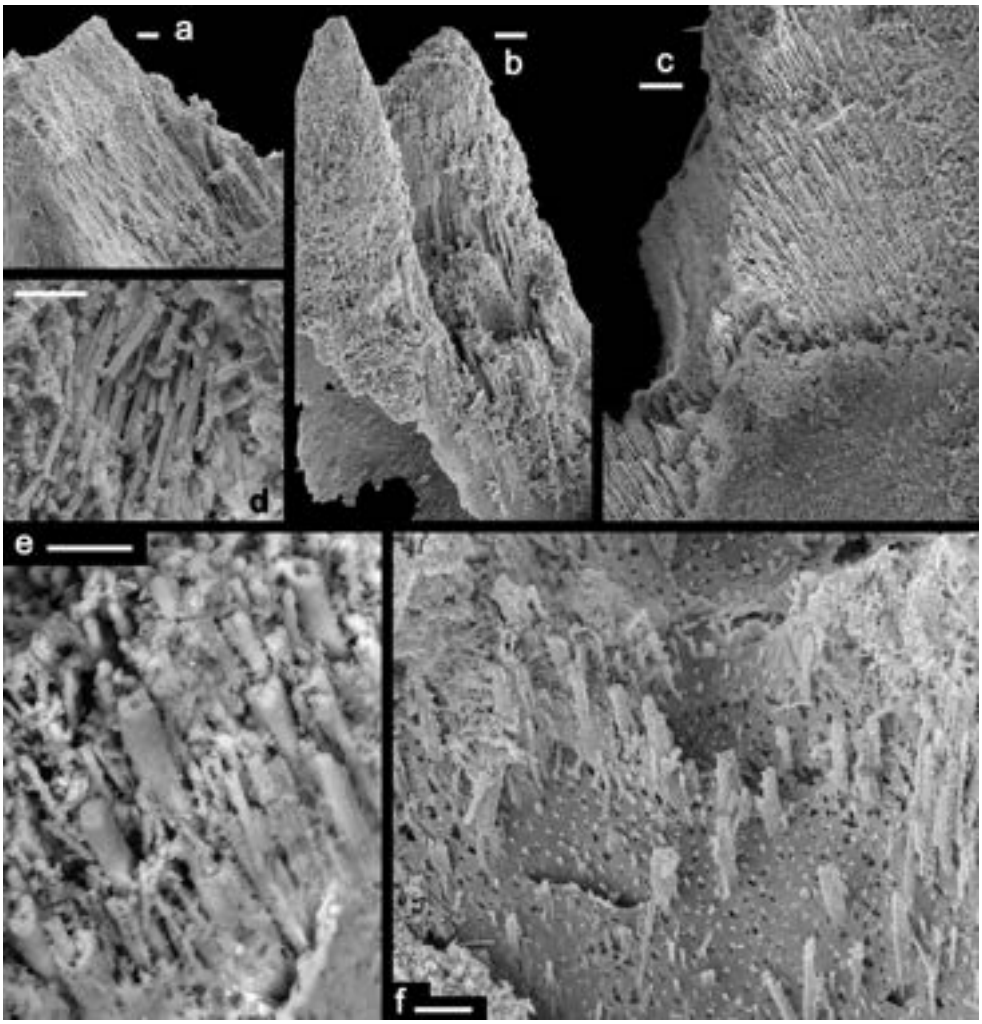

Fig. 4 Microstructure of teeth of isolated archaeostracan gnathal lobes from Puerto Calatraveño area. All images were taken under SEM, and all but **e** are SE images; **e** is a BSE image. Note fibrous microstructure, and the presence of fibres of different thickness. **a** Detail of specimen UEXP880Pu1:015. **b** Detail of specimen UEXP880Pu1:031. **c** Detail of specimen UEXP880Pu1:012. **d** Close up of fibres in specimen UEXP880Pu1:006. **e** Close up of fibres in specimen UEXP880Pu1:001. Some fibres appear tubular or consisting of thinner fibres. **f** Close up of fibres in the base of teeth of specimen UEXP880Pu1:020; note how fibres cut across a thin horizontal/oblique layer; some fibres appear to consist of thinner fibres. Scale bars represent 20 μm in **a**–**c** and 10 μm in **d**–**f**

Therefore, it is likely that the fossils preserve to some extent the original microstructure of the archaeostracan mandibles.

The mandibles are phosphatic (calcium phosphate) in composition (all studied specimens were analysed with EDS, and BSE imaged; some relevant images are illustrated in Figs. 3d, g and h and 5a). Some specimens have distinct organic layers or patches (clearly observable in BSE images; Figs. 3h and 5a) and carbon is generally an abundant element in the specimens analysed with EDS. The general abundance of carbon likely marks the presence of organic matter but, apart from those specimens with distinct organic layers or patches, the precise distribution of the organic matter in the mandible microstructure is not evident. Some specimens have small silica patches apparently integrated into the phosphatic surface (Figs. 3d and g and 5a). Similar patches occur as well in the originally phosphatic conodonts (Fig. 5b), although tend to be more superficial, which may be related to conodonts having a less porous microstructure. Small quantities of other minerals, particularly phyllosilicates and iron oxides (likely replacing pyrite; Fig. 5a) occur as well on the surface of some specimens, but the occurrence of these minerals is almost ubiquitous in fossil samples.

Secondary phosphatization is prevalent in the limestone samples where the studied archaeostracan mandibles occur. It occurs in graptolites (which are preserved as phosphatized internal moulds, partially preserving their organic wall; 5c), three dimensionally preserved guts/coprolites of unidentified metazoans, internal and external moulds of gastropods and bivalves (Fig. 5e, h), cephalopod septa (Fig. 5f, i) and, rarely, in echinoderm plates (Fig. 5d, g). However, in the examples where phosphate is (very likely) "replacing" (the actual mechanism of phosphatization is not known) a primary, biogenic mineral (in cephalopod septa and echinoderm plates) the original microstructure is not preserved. Phosphate occurs as 1–2 μm cubes (Fig. 5g, i), identical to those present in the moulds (Fig. 5h), where phosphate is clearly diagenetic. On the contrary, in the archaeostracan mandibles, a fine, distinct, and likely original microstructure is preserved (see Fig. 4). Additionally, the similarities between the microstructue of the fossil mandibles and the fibrous chitinous scaffolds that characterize the cuticle of

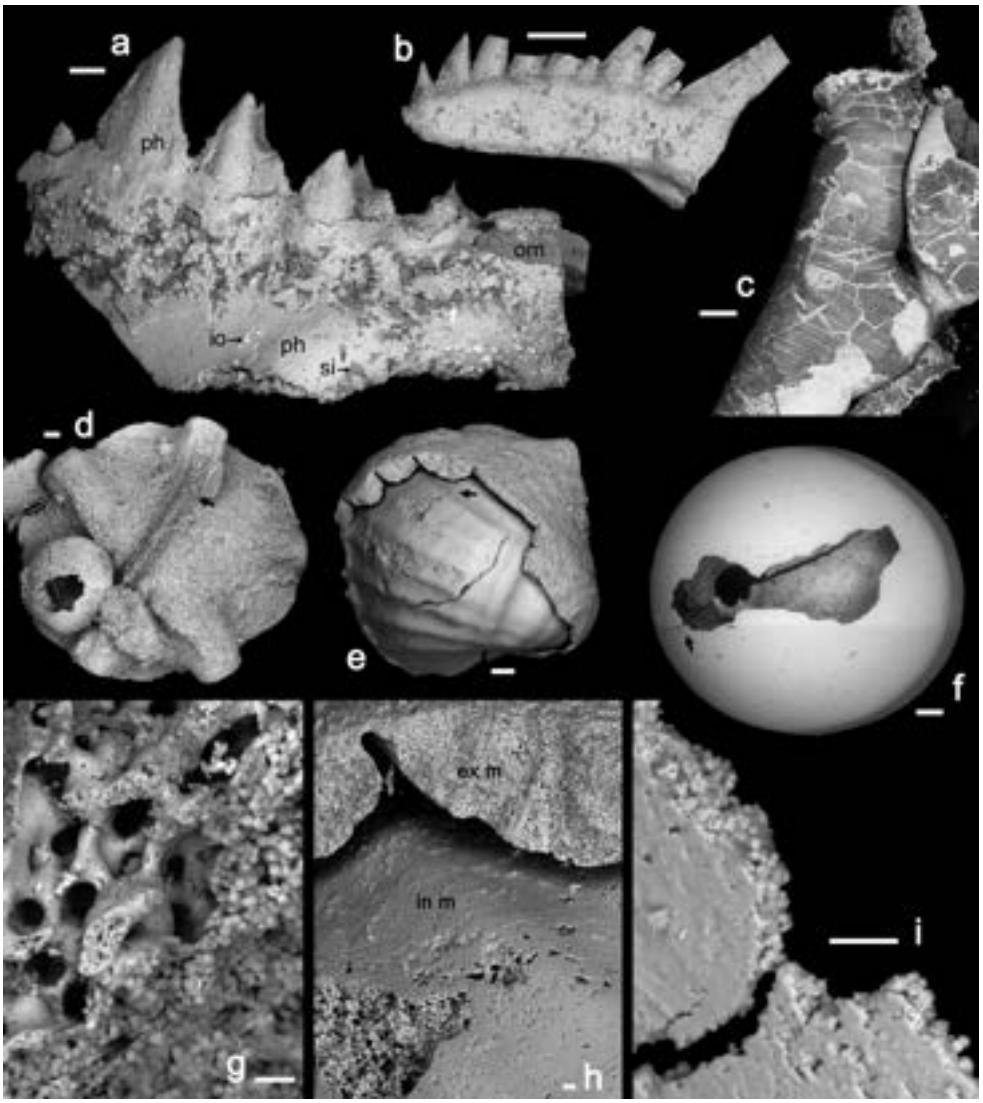

Fig. 5 BSE images illustrating composition and microstructure of an archaeostracan gnathal lobe (**a**) and various originally and secondarily phosphatic fossils from the same samples, Puerto Calatraveño area. All illustrated fossils have a phosphatic composition (light grey), but other minerals and organic matter are also present in some of them (see below). **a** Specimen UEXP880Pu1:012 (also illustrated, in different angle, in Fig. 2a, b), an almost complete archaeostracan gnathal lobe; main composition of the fossil is calcium phosphate (ph, light grey), but it also contains siliceous patches (silica/phyllosilicates; si, in darker grey), iron oxyde crystals (io, white) and "blocks"/crackled layers of organic matter (om, darkest grey). **b** Originally phosphatic conodont (specimen UEXP880Pu1:038) with small siliceous patches. **c** Graptolite (specimen UEXP880Pu1:039) preserved as a phosphatic internal mould with original organic matter partly preserved. **d** Secondarily phosphatized echinoderm ossicle (specimen UEXP880Pu1:040); black arrow points to area magnified in **g**. **e** Phosphatic internal and external moulds of a molluscan shell (specimen UEXP880Pu1:041), original shell dissolved; black arrow points to area magnified in **h**. **f** Secondarily phosphatized cephalopod septum (specimen UEXP880Pu1:042); black arrow points to area magnified in **i**. **g** Magnified area of echinoderm ossicle in **d**; stereom secondarily "replaced" by phosphate (the actual mechanism of phosphatization of the stereom is not known); note phosphate microstructure is in the form of µm-sized cubes. **h** Magnified area of molluscan moulds in e; phosphate microstructure is in the form of small, µm-sized cubes. **i** Thin walled, ca. 5 µm thick, cephalopod septum (magnified from f) made of tiny, ca. 1–2 µm large, phosphatic cubes (the actual mechanism of phosphatization of the, likely calcareous, septum is not known). Scale bars represent 100 µm in **a**–**f** and 10 µm in **g**–**i**. Abbreviations: ex m: external mould; in m: internal mould; io: iron oxide; om: organic matter; ph: calcium phosphate; si: silica/phyllosilicates

modern arthropods strongly support the identification of this microstructure as original. This suggests that the phosphatic composition of the studied mandibles is also original. No calcium carbonate was detected in the mandibles; however, the samples were obtained by acetic acid dissolution and, therefore, are decalcified. Therefore, it is possible that calcium carbonate was also a component of the original mandibles.

Our results support the hypothesis that the trait of incorporating phosphate in wear prone surfaces was present in

early, Paleozoic malacostracans and support the hypothesis of a dual calcium phosphate/carbonate mineralization system evolving early in arthropods (Bentov et al., 2016a, b). They also prompt a re-evaluation of previously described phospatic cuticles in archaeostracans (e.g. Vannier et al., 2003; Briggs et al., 2011; Jones et al., 2015; Wendruff et al., 2020; Liu et al., 2023), considering the possibility of original (instead of diagenetic) phosphatization, particularly, since the existing data strongly point to a weak phosphatic mineralization in archaeostracan cuticle.

As mentioned above, current data supports an originally phosphatic cuticle in other early arthropods, particularly phosphatocopines, aglaspidids and at least some bradoriids (Lin et al., 2011; see also Streng et al., 2008). Since the trait appears phylogenetically scattered, Lin at al. (2011) concluded that a phosphatic cuticle is likely to have evolved several times among arthropods. However, the convergent evolution of a phosphatic cuticle (in the sense of phosphate being its predominant mineral), is compatible with a dual calcium phosphate/carbonate mineralization system having evolved early in the arthropod lineage. In fact, the origination of such a dual system, capable of "fine tuning" the proportion of both components early in the arthropod lineage (Bentov et al., 2016a), makes the independent development of a phosphatic cuticle in several arthropod groups more likely.

Acknowledgements MMM acknowledges financial support to the Spanish Ministerio de Ciencia e Innovación provided through grant PID2021-125585NB-I00. VLR was funded by the Fellowship 2021.06877.BD of the Fundação para a Ciência e Tecnologia. We thank the two anonymous reviewers for their constructive comments.

Funding Open Access funding provided thanks to the CRUE-CSIC agreement with Springer Nature.

Declarations

Conflict of interest on behalf of all authors, the corresponding author states that there is no conflict of interest.

References

Apalategui Isaza, O., Higueras Higueras, P., Pérez Llorente, F., & Roldán García, F. J. (1985a). *Mapa Geológico De España E. 1.50.000. Espiel. Memoria*. Instituto Geológico y Minero de España.

Apalategui Isaza, O., Roldán García, F. J., & Pérez Llorente, F. (1985b). *Mapa Geológico De España E. 1.50.000. Espiel. Cartografía*. Instituto Geológico y Minero de España.

Bentov, S., Zaslansky, P., Al-Sawalmih, A., Masic, A., Fratzl, P., Sagi, A., Berman, A., & Aichmayer, B. (2012). Enamel-like apatite crown covering amorphous mineral in a crayfish mandible. *Nature Communications*, *3*, 839. https://doi.org/10.1038/ncomms1839

Bentov, S., Abehsera, S., & Sagi, A. (2016a). The mineralized exoskeletons of crustaceans. In E. Cohen, & B. Moussian (Eds.), *Extracellular Composite matrices in Arthropods* (pp. 137–163). Springer. https://doi.org/10.1007/978-3-319-40740-1

Bentov, S., Aflalo, E. D., Tynyakov, J., Glazer, L., & Sagi, A. (2016b). Calcium phosphate mineralization is widely applied in crustacean mandibles. *Scientific Reports*, *6*(22118). https://doi.org/10.1038/srep22118

Briggs, D. E. G., Sutton, M. D., Siveter, D. J., & Siveter, D. J. (2004). A new phyllocarid (Crustacea: Malacostraca) from the Silurian Fossil-Lagerstätte of Herefordshire, UK. *Proceedings of the Royal Society of London B: Biological Sciences, 271*, 131–138.

Briggs, D. E. G., Rolfe, W. D. I., Butler, P. D., Liston, J. J., & Ingham, J. K. (2011). Phyllocarid crustaceans from the Upper Devonian Gogo formation, Western Australia. *Journal of Systematic Palaeontology*, *9*, 399–424.

Broda, K., Collette, J., & Budil, P. (2017). Phyllocarid crustaceans from the late devonian of the Kowala quarry (Holy Cross Mountains, central Poland). *Papers in Palaeontology*, *4*, 67–84.

Cheng, L., Wang, L., & Karlsson, A. M. (2008). Image analyses of two crustacean exoskeletons and implications of the exoskeletal microstructure on the mechanical behaviour. *Journal of Materials Research*, *23*, 2854–2872.

Claus, C. (1880). *Grundzüge Der Zoologie. Zum Wissenschaftlichen Gebrauche. Vol. 1* (4th ed., p. 822). Elwert.

Claus, C. (1888). Über Den Organismus Der Nebaliden Und die systematische Stellung Der Leptostraken. *Arbeiten aus dem Zoologische Institut Der Universität Wien Und Der Zoologischen Station in Triest*, *8*, 1–148.

Collette, J. H., & Hagadorn, J. W. (2010a). Three-dimensionally preserved arthropods from Cambrian lagerstätten of Quebec and Wisconsin. *Journal of Paleontology*, *84*, 646–667.

Collette, J. H., & Hagadorn, J. W. (2010b). Early evolution of phyllocarid arthropods: Phylogeny and systematics of Cambrian–devonian archaeostracans. *Journal of Paleontology*, *84*, 795–820.

Collette, J. H., & Rudkin, D. M. (2010). Phyllocarid crustaceans from the silurian Eramosa lagerstätte (Ontario, Canada): Taxonomy and functional morphology. *Journal of Paleontology*, *84*, 118–127.

Dzik, J. (1980). Isolated mandibles of early palaeozoic phyllocarid Crustacea. *Neues Jahrbuch Für Geologie Und Paläontologie Monatshefte*, *1980(2)*, 87–106.

Edgecombe, G. D., Richter, S., & Wilson, G. D. F. (2003). The mandibular gnathal edges: Homologous structures throughout Mandibulata? *African Invertebrates*, *44*, 115–135.

Hessler, R. R., & Schram, F. R. (1984). Leptostraca as living fossils. In N. Eldredge, & S. M. Stanley (Eds.), *Living fossils* (pp. 187–191). Springer.

Jeppsson, L., Anehus, R., & Fredholm, D. (1999). The optimal acetate buffered acetic acid technique for extracting phosphatic fossils. *Journal of Paleontology*, *3*, 964–972.

Jones, W. T., Feldmann, R. M., & Schweitzer, C. E. (2015). *Ceratiocaris* from the Silurian Waukesha Biota, Wisconsin. *Journal of Paleontology*, *89*, 1007–1021.

Lin, J. P., Ivantsov, A. Y., & Briggs, D. E. G. (2011). The cuticle of the enigmatic arthropod *Phytophilaspis* and biomineralization in Cambrian arthropods. *Lethaia*, *44*, 344–349.

Liu, Y., Fan, R., Zong, R., & Gong, Y. (2023). First occurrence of caryocaridids (Crustacea, Phyllocarida) in the Ordovician of North China. *Palaeogeography Palaeoclimatology Palaeoecology*, *623*, 111638.

Lorenzo, S., Gutiérrez-Marco, J. C., Perrier, V., & Serventi, P. (2020). Yacimientos paleontológicos del Silúrico superior de Hinojosa Del Duque (provincia de Córdoba, Dominio De Obejo-Valsequillo, suroeste de España). *Geogaceta*, *67*, 75–78.

Packard, A. S. Jr. (1879). The Nebaliad Crustacea as types of a new order. *American Naturalist*, *13*, 128.

Richards, A. G. (1951). *The integument of Arthropods*. University of Minnesota Press.

Richter, S., Møller, O. S., & Wirkner, C. S. (2009). Advances in crustacean phylogenetics. *Arthropod Systematics & Phylogeny*, *67*, 275–286.

Rolfe, W. D. I. (1962). The cuticle of some middle silurian ceratiocaridid Crustacea from Scotland. *Palaeontology*, *5*, 30–51.

Rolfe, W. D. I. (1969). Phyllocarida. In R. C. Moore (Ed.), *Treatise of invertebrate paleontology, Part R, Arthropoda, vol. 4* (pp. 296–331). Geological Society of America & University of Kansas.

Rolfe, W. D. I. (1981). Phyllocarida and the origin of the Malacostraca. *Géobios*, *14*, 17–27.

Schülke, I., & Riemann, F. (2002). Phyllocarid remains (Malacostraca, Crustacea) from the basal famennian (late devonian) of the Montagne Noire (Southern France). *Paläontologische Zeitschrift*, *76*, 201–213.

Schwentner, M., Richter, S., Rogers, D. C., & Giribet, G. (2018). Tetraconatan phylogeny with special focus on Malacostraca and Branchiopoda: highlighting the strength of taxon-specific matrices in phylogenomics. *Proceedings of the Royal Society of London B: Biological Sciences, 285*, 20181524. https://doi.org/10.1098/rspb.2018.1524

Streng, M., Ebbestad, J. O., & Moczydlowska, M. (2008). A *Walcottella*-like bradoriid (Arthropoda) from the lower Cambrian of Sweden. *GFF*, *130*, 11–19.

Vannier, J., Racheboeuf, P. R., Brussa, E. D., Williams, M., Rushton, A. W. A., Servais, T., & Siveter, D. J. (2003). Cosmopolitan arthropod zooplankton in the ordovician seas. *Palaeogeography Palaeoclimatology Palaeoecology*, *195*, 173–191.

Wendruff, A. J., Babcock, L. E., Kluessendorf, J., & Mikulic, D. G. (2020). Paleobiology and taphonomy of exceptionally preserved organisms from the Waukesha Biota (silurian), Wisconsin, USA. *Palaeogeography Palaeoclimatology Palaeoecology*, *546*, 109631.